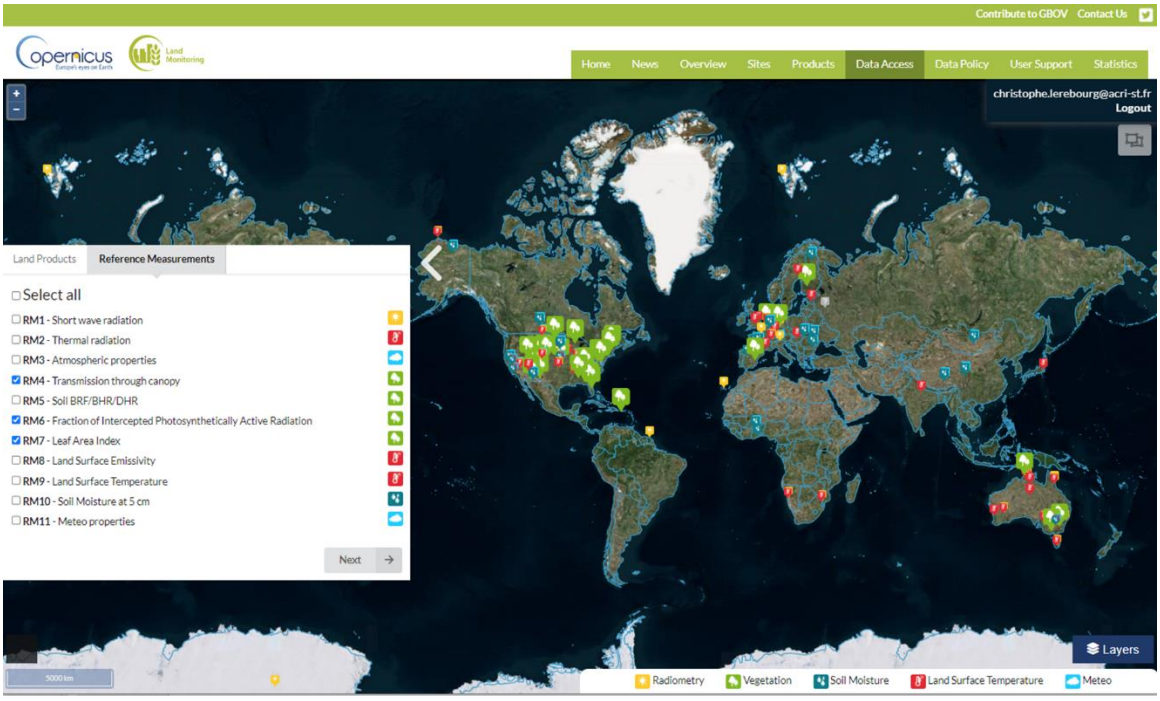
Ground-Based Observations for Validation (GBOV) of Copernicus Global Land Products

Algorithm Theoretical Basis Document - Vegetation Products

LP3 (LAI), LP4 (FAPAR) and LP5 (FCOVER)



Ref. : GBOV_ATBD_LP3-LP4-LP5

Version: 3.2

Date: 11/12/2024

Framework Contract ref.: 941837

© 2017-2024 ACRI-ST

Signatures

	Name	Company	Signature
Book captain	Christophe Lerebourg	ACRI-ST	
Authors	Luke Brown Harry Morris Jadunandan Dash Rémi Grousset	University of Southampton ACRI-ST	
Reviewer	Christophe Lerebourg	ACRI-ST	

Distribution list

Company	To
	Public document

Change log

Version	Date	Changes
3.2	11/12/2024	Updates after external review
3.1	18/12/2023	Update with the new computation approach for the upscaling and the uncertainty computation. Introduction of ICOS sites
3.0	14/09/2021	Updated version delivered at the last milestone of the GBOV SC#10 – Component 1 – Year 4, to reflect implementation of new LP generation algorithm
2.0	18/11/2019	Updated version delivered at the last milestone of the GBOV SC#4 – Component 1 – Year 2
1.2	05/12/2018	Minor corrections from University of Southampton
1.1	14/11/2018	Updated version for the SC#2 closure
1.0	26/09/2018	Initial version delivered at the last milestone of the GBOV SC#2 – Component 1 – Year 1

© 2017-2024 ACRI-ST

Table of contents

1 INTRODUCTION ---- 5
1.1 CONTEXT ---- 5
1.2 SCOPE OF THE DOCUMENT ---- 5
1.3 STRUCTURE OF THE DOCUMENT ---- 5
1.4 ACRONYMS ---- 5

2 SCIENTIFIC BACKGROUND ---- 7
2.1 DEFINITION OF LAND PRODUCTS (LPS) ---- 7
2.1.1 LP3: Leaf area index (LAI) ---- 7
2.1.2 LP4: Fraction of absorbed photosynthetically active radiation (FAPAR) ---- 8
2.1.3 LP5: Fraction of vegetation cover (FCOVER) ---- 9
2.2 UPSCALING TECHNIQUES ---- 9
2.3 CRITERIA FOR ALGORITHM DESIGN ---- 10

3 DESCRIPTION OF THE ALGORITHM ---- 11
3.1 ALGORITHM OUTLINE ---- 11
3.1.1 Input ---- 12
3.1.2 Output ---- 12
3.2 ALGORITHM CHANGES FROM V2.0 ---- 12
3.3 CHANGES IN VERSION 3 SUBVERSIONS ---- 13
3.4 REFERENCE MEASUREMENT (RM) PROCESSING ---- 14
3.4.1 Quality control ---- 14
3.4.2 Combining reference measurements (RMs) ---- 14
3.5 PROCESSING OF HIGH SPATIAL RESOLUTION IMAGERY ---- 16
3.5.1 Data sources ---- 16
3.5.2 Computation of OLI viewing and illumination angles ---- 16
3.5.3 Satellite pixels filtering ---- 16
3.5.4 Execution of the Simplified Level 2 Prototype Processor ---- 16
3.5.5 Derivation of calibration functions ---- 17
3.6 APPLICATION OF CALIBRATION FUNCTIONS TO DERIVE LAND PRODUCTS (LPS) ---- 21
3.7 QUALITY INDICATORS AND FLAGS DERIVATION ---- 21
3.8 UNCERTAINTIES DERIVATION ---- 22
3.9 AGGREGATION AND REPROJECTION OF LAND PRODUCTS (LPS) ---- 23

4 DISCUSSION ---- 24
4.1 TRANSFER FUNCTION DISCUSSION ---- 24
4.2 AGGREGATION METHODS DISCUSSION ---- 24

5 RECOMMENDATIONS FOR USE OF LAND PRODUCTS (LPS) ---- 25

© 2017-2024 ACRI-ST

List of figures

Figure 1: Diagram illustrating the 'two-stage' or 'bottom-up' approach applied to derive LPs from RMs. 10

Figure 2: Flow diagram illustrating the logic of the algorithm. 11

Figure 3: LAI transfer functions for NEON and GBOV 19

Figure 4: FAPAR transfer functions for NEON and GBOV 19

Figure 5: Fcover transfer functions for NEON and GBOV 19

Figure 6: ICOS transfer functions for LAI (top left), FAPAR (top right) and FCOVER (bottom) 20

List of tables

Table 1: Definition of LAI quantities. 7

Table 2: Definition of FAPAR quantities. 8

Table 3: Definition of FCOVER quantities. 9

Table 4: Combination strategies adopted where RMs derived from both upward and downward facing DHP images are provided in a given ESU 15

Table 5: Uncertainty propagation calculations for combined RMs, where RMs derived from both upward and downward facing DHP images are provided in a given ESU. 15

Table 6: ESU measurement footprints and associated window sizes used to match RMs with OLI and MSI pixels. 17

Table 7: Physical and/or practical minima and maxima within which derived LP values are constrained 21

Table 8: Performance metrics calculated using leave-one-out cross validation, where $\boldsymbol{yi}$ is the predicted value, $\boldsymbol{yi}$ is the observed value, $\boldsymbol{y}$ is the mean of observed values, and $\boldsymbol{n}$ is the number of observations. 21

© 2017-2024 ACRI-ST

1 Introduction

1.1 Context

The Ground-Based Observations for Validation (GBOV) service aims to develop and distribute robust in situ datasets from a selection of ground-based monitoring sites for a systematic and quantitative validation of EO land products. The EO land products of particular interest are those from the Copernicus Global Land Service (CGLS).

1.2 Scope of the document

This algorithm theoretical basis document (ATBD) describes the algorithm used to derive land products (LPs):

- LP3 – leaf area index (LAI);
- LP4 – fraction of absorbed photosynthetically active radiation (FAPAR);
- LP5 – fraction of vegetation cover (FCOVER).

1.3 Structure of the document

This document contains the following sections:

- This section introduces the document;
- Section 2 provides the scientific background to the algorithm;
- Section 3 provides a detailed description of the algorithm itself;
- Section 4 provides a discussion about the method and its weaknesses;
- Section 5 provides recommendations for the use of LPs;
- Annex A provides the scientific references cited in this document.

1.4 Acronyms

The definition of the acronyms used in this document is provided hereafter:

ANN	Artificial neural network
ATBD	Algorithm theoretical basis document
BRDF	Bidirectional reflectance distribution function
CEOS	Committee on Earth Observation Satellites
DHP	Digital hemispherical photography
ECV	Essential climate variable
EO	Earth Observation
ESU	Elementary sampling unit

© 2017-2024 ACRI-ST

FCOVER	Fraction of vegetation cover
FAPAR	Fraction of absorbed photosynthetically active radiation
FIPAR	Fraction of intercepted photosynthetically active radiation
GAI	Green area index
GAI_e	Effective green area index
GBOV	Ground-Based Observations for Validation (GBOV) of Copernicus Global Land Products
GUM	Guide to the Expression of Uncertainty in Measurement
ICOS	Integrated Carbon Observation System
JRC	Joint Research Centre
LAI	Leaf area index
LAI_e	Effective leaf area index
LaSRC	Landsat Surface Reflectance Code
LP	Land product
LPV	Land Product Validation
MSI	Multispectral Instrument
NEON	National Ecological Observatory Network
NPV	Non-photosynthetic vegetation
OLI	Operational Land Imager
OLS	Ordinary least squares
PAI	Plant area index
PAI_e	Effective plant area index
PAR	Photosynthetically active radiation
PPFD	Photosynthetic photon flux density
PROSPECT	Leaf Optical Properties Spectra
RM	Reference measurement
RMSE	Root mean square error
RRMSE	Relative RMSE
RTM	Radiative transfer model
SAIL	Scattering by Arbitrarily Inclined Leaves
S2GM	Sentinel-2 Global Mosaic service
SL2P	Simplified Level 2 Prototype Processor
T_{canopy}	Transmission through the Canopy
WGCV	Working Group on Calibration and Validation
WGS84	World Geodetic System 1984

© 2017-2024 ACRI-ST

2 Scientific background

2.1 Definition of land products (LPs)

The definitions of the considered LPs are provided in the following sub-sections:

2.1.1 LP3: Leaf area index (LAI)

LAI corresponds to the one-sided leaf area per unit of ground surface area and describes the amount of leaf material in a vegetation canopy. It is an important descriptor of canopy structure, determining the size of the interface for biogeochemical and energy exchange between vegetation and the atmosphere. As such, it is designated an Essential Climate Variable (ECV). LAI is a dimensionless quantity that typically varies between the values of 0 and 10, and as an intrinsic property of the canopy, is not dependent on observation conditions such as illumination geometry (although when estimated using optical in situ measurement techniques, independence from illumination geometry cannot be assumed). An LAI of 0 means that there is no leaf at all, and a LAI of 10 means that if you look at a surface of ʎ m^2, the total surface area of all the leaves directly above this area is 10 times ʎ m^2. [36]

The term green area index (GAI) is sometimes used to refer to measurements of green elements only, whereas the term plant area index (PAI) refers to measurements that also incorporate non-photosynthetic vegetation (NPV) elements such as stems and branches. Then, PAI = GAI + NPV. It is difficult to collect GAI as any measurement will always have the component of NPV. However, to accurately measure GAI for deciduous plants, one approach is to find the NPV component during the winter season and subtract that from PAI. Note that if the effects of foliage clumping are not accounted for, the measurement is considered an effective one, which will underestimate the true value (Table 1).

Table 1: Definition of LAI quantities.

	All canopy elements incorporated	Foliage elements only	Green elements only (no senescent material)
Foliage clumping not accounted for	Effective PAI (PAI_e)	Effective LAI (LAI_e)	Effective GAI (GAI_e)
Foliage clumping accounted for	PAI	LAI	GAI

LP3 is based on RM7, and further information on its derivation is provided in the associated ATBD (GBOV-ATBD-RM4-RM6-RM7). **Note that because the in-situ measurements may be sensitive to all elements of the canopy, the resulting estimates should strictly be termed PAI (as opposed to LAI or GAI). Both PAI and PAI_e are provided.**

© 2017-2024 ACRI-ST

For simplicity, the terms LAI and LAI_e are used interchangeably with PAI and PAI_e when referring to LP3.

2.1.2 LP4: Fraction of absorbed photosynthetically active radiation (FAPAR)

FAPAR corresponds to the amount of Photosynthetically Active Radiation (PAR) that is absorbed by the canopy. PAR is defined as the radiation at wavelengths of between 400 nm and 700 nm and is measured as photosynthetic photon flux density (PPFD) in units of $\mu mol\ m^{-2}\ s^{-1}$. It is the radiation within this region of the electromagnetic spectrum that is absorbed by photosynthetic pigments in plants for the purposes of photosynthesis. FAPAR is a dimensionless quantity that ranges from 0 to 1 and depends on illumination geometry and the proportion of direct and diffuse radiation. FAPAR is a key variable for monitoring and modelling the primary productivity and energy balance of the terrestrial surface, and as such is designated an ECV. [36]

FAPAR can be defined as instantaneous or temporally averaged depending on the time period over which it is computed, and black-sky or white-sky depending on whether direct or diffuse radiation is considered. Black-sky refers to the case when the incoming radiation flux is unidirectional, without any atmospheric effects. On the other hand, white-sky is when the incoming radiation flux is completely diffuse. The terms green and foliage FAPAR are sometimes used to refer to the fraction of PAR absorbed by photosynthetic canopy elements only, whereas FAPAR contains the contribution of both foliage and NPV elements such as stems and branches (Table 2).

Table 2: Definition of FAPAR quantities.

	All canopy elements incorporated	Foliage elements only	Green elements only (no senescent material)
Direct radiation	Black-sky FAPAR	Black-sky foliage FAPAR	Black-sky green FAPAR
Diffuse radiation	White-sky FAPAR	White-sky foliage FAPAR	White-sky green FAPAR

LP4 is based on RM6, which corresponds to the fraction of intercepted PAR (FIPAR). Further information on its derivation is provided in the associated ATBD (GBOV-ATBD-RM4-RM6-RM7). **The difference between FAPAR and the fraction of intercepted PAR (FIPAR) is considered minimal in most circumstances, making in situ measurements of FIPAR suitable for validating satellite-derived FAPAR products in the absence of in-situ FAPAR data [1], [2]**. The validity of this assumption was investigated by [3], who demonstrated that differences of up to 0.1 may occur over very bright backgrounds such a snow, but that differences are minimal under usual conditions (e.g. when a vegetated understory is present). Under typical circumstances, [3] concluded that these differences can be neglected in the overall

© 2017-2024 ACRI-ST

uncertainty budget. Similar results are presented by [4]. Thus, for the production of LP4, FIPAR is considered equivalent to FAPAR, and the terms are used interchangeably for simplicity. **Note that LP4 corresponds to the instantaneous black-sky definition at 10:00 AM local solar time and represents FAPAR (as opposed to foliage or green FAPAR) as the in-situ measurements may be sensitive to all elements of the canopy. 10:00 AM local solar time means two hours before solar noon (when the sun is at its highest point in the sky) but may not necessarily be 10:00 AM on the local clock.**

2.1.3 LP5: Fraction of vegetation cover (FCOVER)

FCOVER corresponds to the amount of the ground surface that is covered by vegetation when viewed from nadir, thus acting as an indicator of the spatial extent of vegetation [36]. It is a dimensionless quantity that varies from 0 to 1, and as an intrinsic property of the canopy, is not dependent on observation conditions such as illumination geometry (although when estimated using optical in-situ measurement techniques, independence from illumination geometry cannot be assumed). The terms green and foliage FCOVER are sometimes used to refer to the fraction of ground covered by photosynthetic canopy elements only (Table 3).

Table 3: Definition of FCOVER quantities.

All canopy elements incorporated	Foliage elements only	Green elements only (no senescent material)
FCOVER	Foliage FCOVER	Green FCOVER

LP5 is based on in-situ measurements of FCOVER, and further information on their derivation is provided in the associated ATBD (GBOV-ATBD-RM4-RM6-RM7). **Note that LP5 represents FCOVER (as opposed to foliage or green FCOVER) as the in-situ measurements may be sensitive to all elements of the canopy.**

2.2 Upscaling techniques

Major challenges in the validation of operational satellite-derived vegetation products are their moderate spatial resolution and the heterogeneity of the terrestrial landscape. The Copernicus Global Land Service products are produced at a spatial resolution of between 300 m and 1 km, whilst individual in-situ measurements are typically point-based covering a smaller area. Over the last few decades, techniques have been developed to bridge this scale gap, typically making use of high spatial resolution imagery to match the scale of elementary sampling unit for upscaling, which means for the transition from a point-based measurement to a larger scale. Here “high spatial resolution imagery” refers to satellite data with a finer spatial resolution (typically 20 or 30 meters) compared to the land product (typically 300 meters). These techniques, which are endorsed by the Land Product Validation (LPV) sub-group of the Committee on Earth Observation Satellites (CEOS) Working Group on Calibration

© 2017-2024 ACRI-ST

and Validation (WGCV), are often referred to as the 'two stage' or 'bottom up' approach [5], [6]

Within the 'two stage' or 'bottom up' approach, individual in-situ measurements are made within Elementary Sampling Units (ESUs) that approximate the extent of a pixel of the high spatial resolution imagery used for upscaling. Several within-ESU sampling strategies can be defined, depending on vegetation density and homogeneity, including square, cross, and transect patterns [5]–[7]. Once collected, alternative methods are then available to associate ESU-level in situ measurement values (i.e. RMs) to the high spatial resolution imagery itself. These methods include establishing empirical transfer functions, in addition to the inversion of radiative transfer models (RTMs) [5]–[10]. Using these methods, a high spatial resolution map of the LP of interest can be produced, which can then be aggregated to the required spatial resolution for the purposes of product validation (Figure 1). This transition from point-based in-situ measurements to high spatial resolution imagery-based land product is called "upscaling".

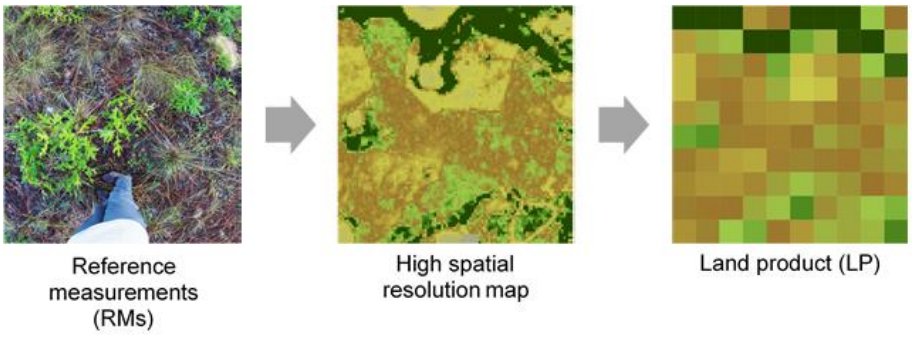


Figure 1: Diagram illustrating the 'two-stage' or 'bottom-up' approach applied to derive LPs from RMs.

2.3 Criteria for algorithm design

Criteria for the design of the algorithm are outlined below:

- Given the large number of LPs that are to be produced, the algorithm should be computationally efficient, enabling operational implementation;
- The algorithm should be applicable over all vegetation types covered by the selected sites;
- In addition to the value of each LP, quality indicators and quantitative estimates of uncertainty should be provided, allowing users to assess its fitness for purpose.

© 2017-2024 ACRI-ST

3 Description of the algorithm

3.1 Algorithm outline

A new method to derive LPs has been implemented as of V3.0 of the algorithm, based on feedback from the user community. Whilst LPs derived using V1.0 and V2.0 have proven useful for several validation exercises [11], [12], several shortcomings were also identified, including weak predictive power over some sites, limited extrapolation capabilities when transfer functions were applied to images acquired outside the time period represented in their training data, and poorly resolved seasonality in some cases [12]. Based on the approach described in [13] and incorporating several improvements, the V3.0 algorithm takes as input the RMs collected over a given site, in addition to a series of high spatial resolution images. Calibration functions are then derived between RMs and RTM-based retrievals, enabling high spatial resolution maps of each RM to be produced. Finally, these maps are aggregated and reprojected to the spatial resolution and product grid of the Copernicus Global Land Service products (Figure 2).

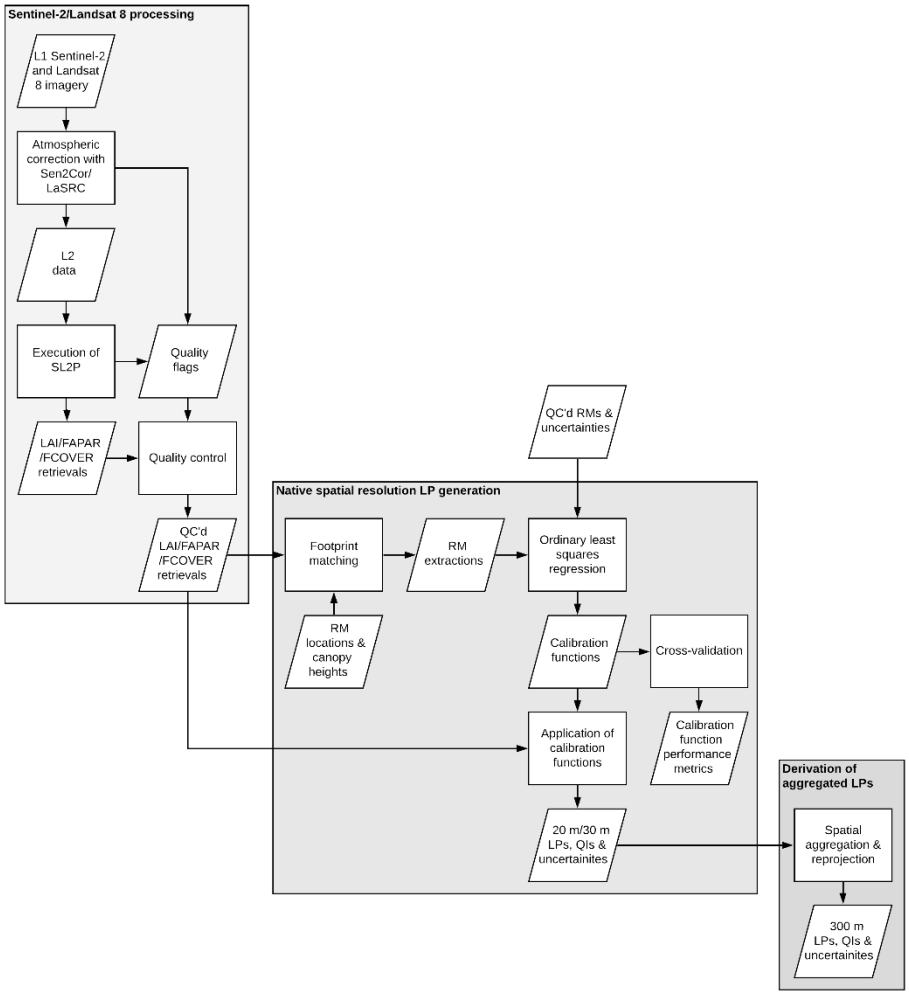


Figure 2: Flow diagram illustrating the logic of the algorithm.

© 2017-2024 ACRI-ST

The use of calibrated RTM-based retrievals as opposed to vegetation index-based multitemporal transfer functions enables the impact of non-canopy factors that perturb the vegetation index-biophysical variable relationship to be reduced [14]. For example, as viewing and illumination angles are an explicit input, seasonal variations in sun-sensor geometry can be better accounted for, whilst the variety of soil spectra used in the RTM simulations helps reducing the impact of the soil background [14]. To maintain computational efficiency, a hybrid method using artificial neural networks (ANNs) trained with RTM simulations was selected as opposed to a pure inversion approach. This method is called SL2P for Simplified Level 2 Prototype Processor.

3.1.1 Input

The input to the algorithm consists of RMs 6, 7 and FCOVER (GBOV-ATBD-RM4-RM6-RM7), in addition to a series of high spatial resolution images over each of the selected sites. Landsat OLI and Sentinel2 MSI are the privilege high spatial resolution data used. When enough usable Sentinel 2 data is available for a site, Landsat 8 data is not used for the upscaling (refer to section 2.2). Since 2018, two Sentinel 2 satellites have been in orbit, so in most cases Sentinel 2 data is sufficient.

3.1.2 Output

The output of the algorithm consists of at least 3 km x 3 km map of each LP. Along with the LP value, per-pixel quality indicators and uncertainty estimates are provided. LPs are provided in:

- the native spatial resolution and projection of the imagery used for upscaling (20m)
- a reduced spatial resolution of 300 m, in the native projection (only up to version 3.2)
- a reduced spatial resolution of 300 m reprojected to the World Geodetic System 1984 (WGS84) coordinate system (as used by the Copernicus Global Land Service products [15]).

3.2 Algorithm changes from V2.0

V3.0 of the LP generation algorithm introduced the following changes with respect to V2.0:

- A new upscaling method has been implemented, using a radiative transfer model (RTM) based retrieval approach (the SL2P algorithm detailed in section 3.6.4) as opposed to vegetation index-based multitemporal transfer functions. In the new method, RMs are used to establish calibration functions, which enable biases in the raw RTM-based retrievals to be corrected for [13];

- A footprint matching procedure has been implemented in which RMs are related to the mean of a variable window of OLI/MSI pixels, whose size depends on the ESU measurement footprint at the site in question [13];

- To improve temporal consistency, the constraint for relating RMs to high spatial resolution imagery has been reduced from ± 7 days to ± 5 day [14];

© 2017-2024 ACRI-ST

3.3 Changes in version 3 subversions

The versions of Land Products delivered and available in the current database are v3.0, v3.1, v3.2, v3.3 and v3.4.0.

The only difference between versions v3.0, v3.1 and v3.2 is the transfer function parameters. These are recalculated each year taking into account the new in-situ measurements collected which have enriched the database.

The v3.0 to v3.2, a 95% confidence interval is provided and calculated as:

$$u_{LP} = t * s * \sqrt{\frac{1}{n} + \frac{(sl2p_{LP} - sl2p_{mean})^2}{(n-1) * (sl2p_{std})^2}}$$

Where:

- t is the percentage point function of the students t test at 95% confidence.
- s is the standard estimates of the error derive from the calibration function of the SL2P extractions and RM values.
- n is the number of points used to derive the calibration function.
- $sl2p_{LP}$ is the SL2P biophysical variable at the pixel
- $sl2p_{mean}$ is the mean of the SL2P values used for deriving the calibration function
- $sl2p_{std}$ is the standard deviation of the SL2P values used for deriving the calibration function
- u_{LP} is the 95% confidence interval of the final Land Product

Up to version 3.2, the procedure to derive the calibration function was derived through a basic Ordinary Least Square procedure. This procedure did not offer the possibility to account for neither X nor Y uncertainties.

In preparation of version 3.3, several regression procedures have been investigated including Weighted Least Square (WLS) and Orthogonal Distance Regression (ODR). In both cases, the computed uncertainty on the regression coefficient (slope and intercept) are saved for the uncertainty propagation.

- The Weighted Least Square procedure allows to account for the uncertainty on the Reference Measurements (RM). Indeed, the Weighted Least Square method takes as input a weight for each point. Here, a point is a matchup between a RM value and the corresponding SL2P's retrieval overpassing this RM value. The weight for a point x is then derived from the uncertainty of the corresponding RM and is computed as $w_x = \frac{1}{u_x{}^2}$ where u_x is the uncertainty of this RM.
- The Orthogonal Distance regression allows to account for the uncertainty on both the Reference Measurements and the SL2P's retrievals (LAI, FAPAR and FCOVER). The same

© 2017-2024 ACRI-ST

way as for WLS, the weights are $w_{SL2Px} = \frac{1}{u_{SL2Px}{}^2}$ for SL2P's retrievals and $w_{RMx} = \frac{1}{u_{RMx}{}^2}$ for RMs.

See section 3.8 for detailed uncertainty computations. For the V3.4.0 product release the Orthogonal Distance Regression approach was implememented where Weighted Least Square regression was implemented for v3.3 products.

As v3.4.0 products are now derived from satellite data downloaded with S2GM (the Sentinel-2 Global Mosaic Service), which was not the case prior v3.4.0, the parameters were recalculated on satellite data covering 2020-2024, (for some specific sites 2018-2024).

Please note that the current database includes past subversions of version 3. A full archive reprocessing will be considered in 2025.

3.4 Reference measurement (RM) processing

3.4.1 Quality control

Prior to the derivation of calibration functions, the quality indicators associated with each RM are applied to discard any spurious or suspect values. As of the current main version of the algorithm (V3.X), all flagged RMs are discarded. Further details on the RM quality indicators can be found in the ATBD for RMs 4, 6, 7 and FCOVER (GBOV-ATBD-RM4-RM6-RM7).

3.4.2 Combining reference measurements (RMs)

3.4.2.1 Case of NEON and GBOV sites.

NEON and GBOV sites provide Reference Measurements derived from both the under and overstory processed using the Hemipy procedure [37] (further details can be found in the ATBD for RMs 4, 6, 7 and FCOVER, GBOV-ATBD-RM4-6-7 available on https://gbov.land.copernicus.eu/products/). In some cases like grasslands or croplands the sole understory is available. Where RMs derived from both upward and downward facing Digital Hemispherical Photo (DHP) images are provided in a single ESU (i.e. at forest sites where an overstory and understory is present), they are combined to obtain a single value. The combination strategy is specific to each RM, and is equivalent to the one adopted in the Validation of Land European Remote Sensing Instruments (VALERI) project [7] (Table 4). The uncertainties associated with the combined RMs are derived using uncertainty propagation calculations, assuming no correlation between uncertainties (Table 5).

© 2017-2024 ACRI-ST

Table 4: Combination strategies adopted where RMs derived from both upward and downward facing DHP images are provided in a given ESU.

RM	Combination strategy
RM4: T_{canopy}	$T_{canopy} = T_{canopy_{up}} - T_{canopy_{up}} (1 - T_{canopy_{down}})$
RM6: FIPAR	$FIPAR = FIPAR_{up} + (1 - FIPAR_{up}) FIPAR_{down}$
RM7: LAI_e	$LAI_e = LAI_{e_{up}} + LAI_{e_{down}}$
RM7: LAI	$LAI = LAI_{up} + LAI_{down}$
FCOVER	$FCOVER = FCOVER_{up} + (1 - FCOVER_{up}) FCOVER_{down}$

Table 5: Uncertainty propagation calculations for combined RMs, where RMs derived from both upward and downward facing DHP images are provided in a given ESU.

RM	Uncertainty propagation calculation
RM4: T_{canopy}	$u(T_{canopy}) = \sqrt{[(1 - T_{canopy_{up}})\ u(T_{canopy_{down}})]^2 + [(1 - T_{canopy_{down}})\ u(FCOVER_{up})]^2}$
RM6: FIPAR	$u(FIPAR) = \sqrt{[(1 - FIPAR_{up})\, u(FIPAR_{down})]^2 + [(1 - FIPAR_{down})\, u(FIPAR_{up})]^2}$
RM7: LAI_e	$u(LAI_e) = \sqrt{u(LAI_{e_{up}})^2 + u(LAI_{e_{down}})^2}$
RM7: LAI	$u(LAI) = \sqrt{u(LAI_{up})^2 + u(LAI_{down})^2}$
FCOVER	$u(FCOVER) = \sqrt{[(1 - FCOVER_{up})\, u(FCOVER_{down})]^2 + [(1 - FCOVER_{down})\, u(FCOVER_{up})]^2}$

3.4.2.2 ICOS sites

ICOS (Integrated Carbon Observation System) has a different DHP acquisition protocol. DHPs are only acquired on forest sites for overstory. ICOS sites RMs are also derived using the Hemipy procedure [37].

The LPs over ICOS are therefore derived from the sole overstory component.

© 2017-2024 ACRI-ST

3.5 Processing of high spatial resolution imagery

3.5.1 Data sources

To minimise the impact of cloud cover and extend the time-series of LPs, both Landsat 8 OLI and Sentinel-2 MSI data are used in synergy for LP production. These data are freely available, incorporate spectral bands that are sensitive to the biophysical variables of interest, and are provided at a spatial resolution that closely matches the extent of the ESUs over which RMs are computed (20 m to 30 m). As imagery collected at different dates and times is to be utilised within the algorithm and surface reflectance values are required by the RTM-based retrieval approach (SL2P), only L2 products, which have been corrected for geometric, radiometric, and atmospheric effects, are considered. These L2 products are produced using standard operational pre-processing algorithms – namely the Landsat Surface Reflectance Code (LaSRC) in the case of OLI [19], [20], and Sen2Cor in the case of MSI [21]. For OLI data, Collection 2 products are used. For MSI, ESA-produced L2A products are used from December 2018 onwards. Prior to December 2018 (when systematic global L2A production began), L1C products are processed to L2A using Sen2Cor 2.5.5.

3.5.2 Computation of OLI viewing and illumination angles

Whilst L2 MSI products are accompanied with bands providing the viewing and illumination geometry, L2 OLI products are not. However, an angle coefficient metadata file is available, enabling per-pixel viewing and illumination angles to be computed. This is achieved by means of the Landsat 8 Angles Creation Tool [22].

3.5.3 Satellite pixels filtering

Prior to use of the high spatial resolution imagery, the quality indicators provided by LaSRC and Sen2Cor are applied to discard pixels contaminated by cloud, cloud shadow, water, and snow/ice. Thus, only clear, valid pixels are considered.

3.5.4 Execution of the Simplified Level 2 Prototype Processor

From OLI and MSI surface reflectance values (and associated viewing/illumination angles), LAI, FAPAR and FCOVER are retrieved with the Simplified Level 2 Prototype Processor (SL2P) described by [23]. SL2P is a hybrid retrieval algorithm that uses artificial neural networks (ANNs) trained with simulations from the coupled Leaf Optical Properties Spectra (PROSPECT) [24], [25] and Scattering by Arbitrarily Inclined Leaves (SAIL) [26], [27] RTMs. Whilst originally designed for MSI data [23], a version of SL2P compatible with OLI data is also now available [28]. Recent validation efforts have shown SL2P's retrievals to be consistently biased, meaning that calibration functions based on the RMs can successfully be used to correct for these biases [13], [29]. In addition to estimates of biophysical variables, SL2P provides quality flags to identify retrievals where the inputs or outputs are outside the range of the training database. Flagged retrievals are excluded from further analysis.

© 2017-2024 ACRI-ST

3.5.5 Derivation of calibration functions

In order to derive calibration functions, RMs are matched to OLI/MSI pixels on the basis of location and the date of sampling. A temporal constraint of ± 5 days is imposed to ensure stability in vegetation conditions [13], [29]. All available L2A MSI scenes (and Collection 2 L2 OLI when necessary) are considered, provided that the pixels associated with each RM are not discarded when the quality indicators are applied (Section 3.7). To ensure a consistent spatial support, the footprint matching approach described in [13] is adopted. RMs are compared with the mean of a variable window of OLI/MSI pixels, whose size is determined according to the ESU measurement footprint at each site. Footprints are calculated by assuming that the DHP-derived RMs were acquired at shoulder height (1.5 m above the ground) and according to the mean canopy height of the site, such that

$$2\,h\,\tan\theta + l$$

where h is the height between the top of the canopy and the camera (or the ground in the case of sites with only downwards-facing images), θ is the maximum zenith angle of the measurement, and l is the one-sided length of the ESU. The smallest, odd window size containing the entire ESU measurement footprint is selected (Table 6).

Table 6: ESU measurement footprints and associated window sizes used to match RMs with OLI and MSI pixels.

Site code	Mean canopy height (m)	Measurement footprint (m)	OLI window size	MSI window size
BART	23	67.5	3	5
BLAN	1	4.7	1	3
CPER	0.4	4.7	1	3
DSNY	1.5	4.7	1	3
GUAN	10	26.7	3	3
HARV	26	76.9	5	5
JERC	27	80.1	5	7
JORN	0.4	4.7	1	3
MOAB	0.2	4.7	1	3
NIWO	0.2	4.7	1	3
ONAQ	1.2	4.7	1	3
ORNL	28	83.2	5	7
OSBS	23	67.5	3	5
SCBI	35	105.2	5	7
SERC	38	114.6	5	7
STEI	5.5	12.6	3	3

© 2017-2024 ACRI-ST

STER	1	4.7	1	3
TALL	25	73.8	5	5
UNDE	24	70.6	5	5
WOOD	1	4.7	1	3
DELA	30	89.5	5	7
LAJA	0.4	4.7	1	3
SRER	2	4.7	1	3
KONA	1.5	4.7	1	3

Having created a database of RMs and associated SL2P LAI, FAPAR, and FCOVER retrievals, calibration functions are derived using Orthogonal Distance Regression (ODR). The ODR fit computes the coefficients by minimising the sum of squared orthogonal distances between each data point and the model. The uncertainties are accounted for into the weight of each point along the corresponding axis (i.e. the RM axis and the LP axis) and are expressed as $w_{SL2Px} = \frac{1}{u_{SL2Px}{}^2}$ for SL2P's retrievals and $w_{RMx} = \frac{1}{u_{RMx}{}^2}$ for RMs.

Linear calibration functions are adopted, as SL2P's retrievals are expected to be linearly related to the RMs. This expectation has been confirmed by previous validation exercises [13], [28], [29]. Owing to the assumptions of SL2P's retrieval scheme, previous work has demonstrated differing biases over these canopy types [29], [30]. Ideally, calibration function specific to vegetation type might provide a better upscaling function. However, as there were few matchups between RMs and SL2P's retrievals for some vegetation types, it is not possible to process one calibration function per vegetation type, only three separate calibration functions are then derived. One for homogeneous (cultivated crops, grassland/herbaceous, pasture/hay, shrub/scrub) canopies on NEON sites, one for heterogeneous (deciduous forest, evergreen forest, mixed forest and woody wetlands) canopies on NEON and GBOV sites and one for ICOS sites which are all sites with heterogeneous canopies. Two distinct transfer functions are derived for NEON and GBOV heterogenous forest sites and ICOS heterogeneous forest sites, as RMs on ICOS sites are derived using only overstory DHPs and the RMs on NEON sites are derived using overstory and understory DHPs.

The following figures represents the calibration functions derived from ICOS (heterogeneous sites) and NEON/GBOV for both the homogeneous and heterogeneous sites. In each case, three regression lines are plotted: the original transfer function used prior v3.3 (OLS) not taking into account the variable uncertainties and calculated with the Ordinary Least Square regression, the WLS and the ODR regression.

© 2017-2024 ACRI-ST

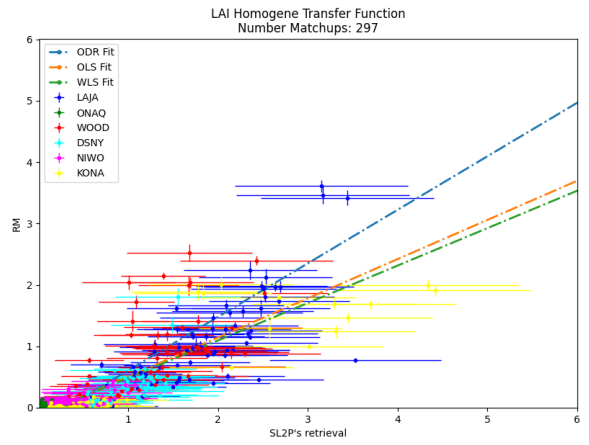
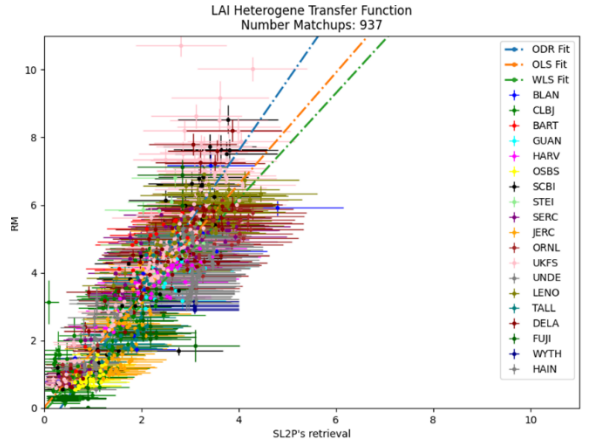
Homogeneous	Heterogeneous
	

Figure 3: LAI transfer functions for NEON and GBOV

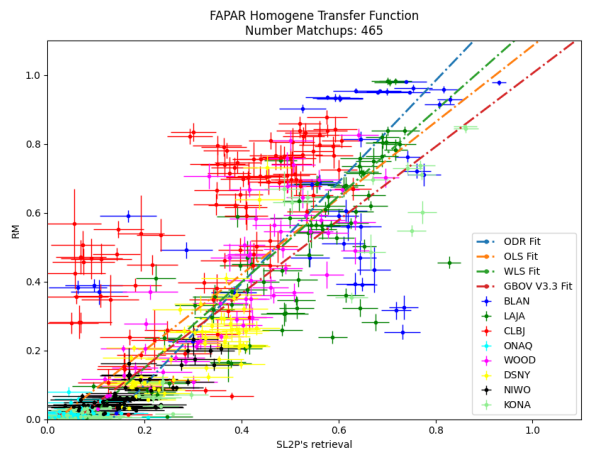
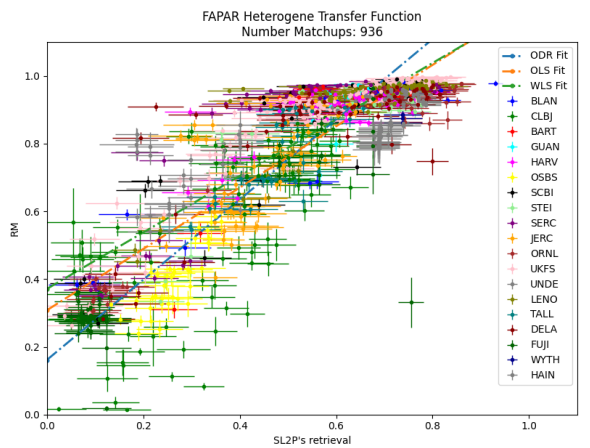
Homogeneous	Heterogeneous
	

Figure 4: FAPAR transfer functions for NEON and GBOV

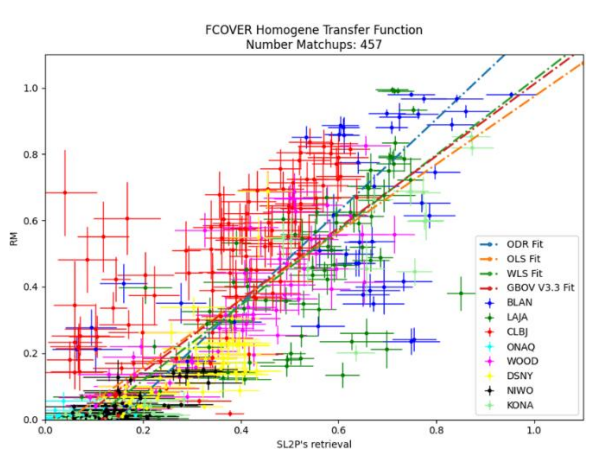
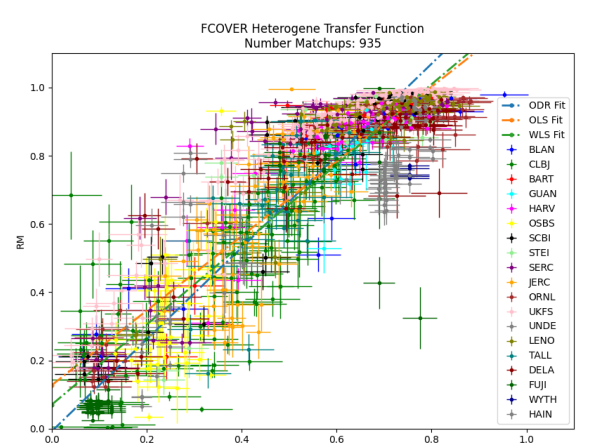
Homogeneous	Heterogeneous
	

Figure 5: Fcover transfer functions for NEON and GBOV

© 2017-2024 ACRI-ST

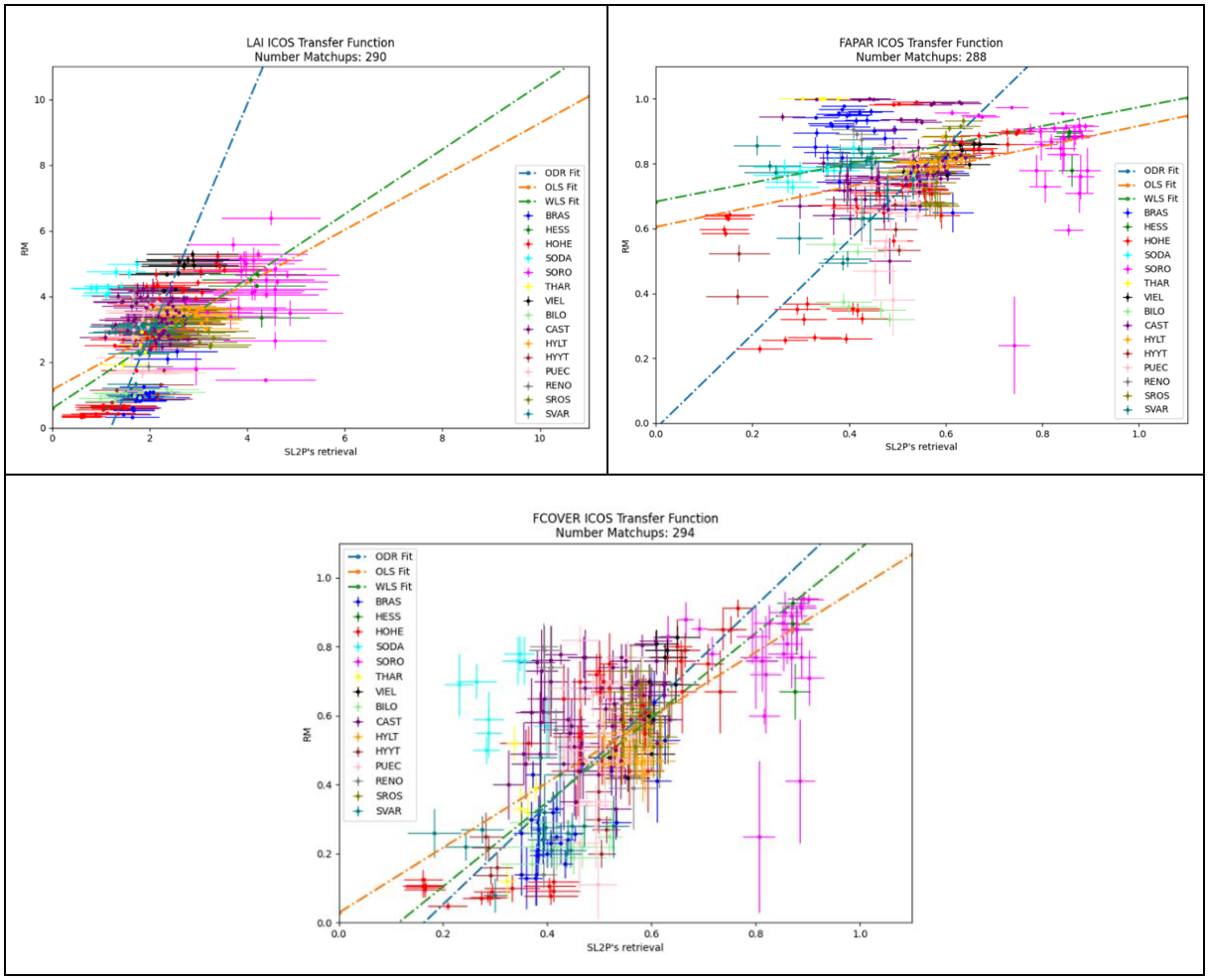


Figure 6: ICOS transfer functions for LAI (top left), FAPAR (top right) and FCOVER (bottom)

As mentioned in section 3.4, the Weighted Least Squares (WLS) and the Orthogonal Distance Regression (ODR) methods to compute the Transfer Functions take into account the uncertainty of the inputs. WLS method takes into account the uncertainties of the RMs and ODR takes into account both the uncertainties of the RMs and the SL2P's retrievals. In those graphs, those uncertainties are displayed as the vertical (for RMs uncertainties) and horizontal (for the SL2P's retrievals uncertainties) lines.

The three ways (OLS, WLS and ODR) of fitting the transfer functions are plotted on those four figures and labelled in the legends. We can therefore notice significant differences between the results of those three fitting methods. As OLS does not account for any of the uncertainties, this solution has been replaced in V3.3 and V3.4.0. In the other hand, ODR is the only fitting method that takes into account all the uncertainties, V3.4.0 products were then derived using it.

It is worth noting that these transfer functions were derived on specific sites mostly in North America and Europe (also a few in Australia), **there is no insurance that they will work on other areas.** Those transfer functions were optimized for those specific sites and were not designed to be used in different conditions.

© 2017-2024 ACRI-ST

3.6 Application of calibration functions to derive land products (LPs)

For each LP and canopy type, the corresponding calibration function is selected and, following the recommendations of the CEOS WGCV LPV sub-group, applied to successive SL2P's retrievals to derive a time series of high spatial resolution reference maps [6]. The selection of the calibration function is made at site-level and the same calibration is applied on each pixel of the site. In applying the calibration functions, only clear, valid pixels are considered (Section 3.7). Unvalid pixels are set to NaN, and the extent of each map is limited to a 3 km x 3 km area covering the site. The derived LP values are constrained within physical and/or practical minima and maxima (Table 7).

Table 7: Physical and/or practical minima and maxima within which derived LP values are constrained.

LP	Minimum	Maximum
LP3: LAI	0	10
LP4: FAPAR	0	1
LP5: FCOVER	0	1

3.7 Quality indicators and flags derivation

In addition to the LP values themselves, quality indicators are provided to allow users to assess their fitness for purpose.

First, to allow the user to estimate the quality of the transfer functions, performance metrics are given. The performance of the calibration function used to derive each LP is assessed using leave-one-out cross validation for prior v3.3 products, which provides information on how well it is likely to generalise to new observations [31]. For v3.3 and v3.4.0 products, the performance metrics are estimated during the regression taking account for the uncertainties of the training dataset. Three performance metrics are calculated: the coefficient of determination (R^2), the root mean square error (RMSE), and the relative root mean square error (RRMSE) (Table 8). These statistics are provided in the README files associated with each LP, as are various descriptive statistics on the data used to establish the calibration function itself.

Table 8: Performance metrics calculated using leave-one-out cross validation, where $\hat{y}_i$ is the predicted value, y_i is the observed value, $\overline{y}$ is the mean of observed values, and n is the number of observations.

Performance metric	Formula
Coefficient of determination (R^2)	$R^2 = 1 - \frac{\sum_{i=1}^{n}(y_i - \hat{y}_i)^2}{\sum_{i=1}^{n}(y_i - \overline{y})^2}$
Root mean square error (RMSE)	$RMSE = \sqrt{\frac{\sum_{i=1}^{n}(\hat{y}_i - y_i)^2}{n}}$

© 2017-2024 ACRI-ST

Relative RMSE (RRMSE)	$RRMSE = \frac{RMSE}{\bar{y}}$

Second, per-pixel quality indicators are provided to identify pixels where LP values are computed by extrapolating beyond the range of the dataset used to establish the calibration function. Indeed, the transfer functions were calibrated on a certain range of values for the SL2P's retrievals, they then must be used only with inputs included in this range. In the same way, the transfer functions were calibrated in a certain range of values for the RMs. If the outputs produced by the transfer function is outside this RMs values range, it must be flagged. In the end, if the input given to the transfer function is outside of the range covered during the calibration, the output is flagged as "input out range" and if the output produced by the transfer function is outside of the range covered during the calibration, this output is flagged as "output out of range".

Third, by the same logic, transfer functions were calibrated over a certain period of the year. It is essential to apply the transfer function on SL2P's retrieval computed on satellite data acquired during this specific period. The period of the year covered by the transfer function used for computing the Land Product and a flag that indicates if the LP is "out of temporal training range" are given in the README file related to that LP.

Finally, a visual quality control is made on Land Products to manually flag the ones with suspicious values. To do so, a time series is computed for each site, each point is a mean of the 9 pixels covering a 3 by 3 pixel zone in the center of the corresponding LP. Doing so, large jumps or falls (which could be due to clouds, water, snow that may have been incorrectly classified as vegetation) can be easily identified and removed from the database.

3.8 Uncertainties derivation

In addition to the LP values and their associated quality indicators, estimates of uncertainty are provided.

Prior to v3.3, per-pixel estimates of LP uncertainty are provided as corresponding to the 95% confidence interval associated with the calibration function used to derive each LP value.

For v3.3 onward, the uncertainty was computed based on the Guide to the Expression of Uncertainty in Measurement (GUM) [35] approach. The GUM has been proposed by the joint committee for guides in metrology and widely used for traceability and uncertainty assessments in measurements.

High spatial resolution land products (LPs) are generated by applying a linear calibration function between individual RMs and the corresponding SL2P's retrievals. The function to be fitted can be written as:

$$X_{RM} = f(X_{SL2P}) = A_X * X_{SL2P} + B_X$$

© 2017-2024 ACRI-ST

where *X* can either be LAI, FAPAR or FCOVER, as derived from RMs (X_{RM}) or from SL2P (X_{SL2P}), and A_X and B_X are the fitting coefficients corresponding to the variable *X*.

There are three different transfer functions (one for forest NEON/GBOV sites, one for croplands and grasslands NEON/GBOV sites and one for ICOS sites) but the same method is used for the three. In order to account for uncertainties propagation in the LP generation process, we use the Orthogonal Distance Regression (ODR) for the calibration, which enables uncertainties in response variables (RMs) and in predicted variables (LPs) to be accounted for in the computations of the regression coefficients by minimising the sum of squared orthogonal distances between each data point and the model.

Subsequently, for each classes, scenes, and LPs, the fit between RMs and SL2P's retrievals generates uncertainties on the fitting coefficients $u(A_X)$ and $u(B_{X)}$, which can be used along with the uncertainties generated by SL2P $u(X_{SL2P})$ to compute the uncertainties on LPs as described in equation above of [35]:

$$u(X_{LP})^2 = \left(\frac{\partial f}{\partial A_X}\right)^2 u(A_X)^2 + \left(\frac{\partial f}{\partial X_{SL2P}}\right)^2 u(X_{SL2P})^2 + \left(\frac{\partial f}{\partial B_X}\right)^2 u(B_X)^2$$

which, applied to the previous equation, leads to:

$$u(X_{LP}) = \sqrt{{X_{SL2P}}^2.u(A_X)^2 + {A_X}^2.u(X_{SL2P})^2 + u(B_X)^2}$$

3.9 Aggregation and reprojection of land products (LPs)

Aggregated LPs are produced at a reduced spatial resolution of 300 m and reprojected to the World Geodetic System 1984 (WGS84) coordinate system used by the Copernicus Global Land Service products [15]. For the continuous LP values and per-pixel uncertainties, mean value downsampling is adopted. An additional band is included to inform the user of the percentage of valid native spatial resolution pixels used in aggregation, so that a threshold may be applied if desired. Pixels flagged as "input out of range" or "output out of range" are ignored during the downsampling of the LP values and uncertainties and are considered as unvalid for the computation of the "percentage of valid native spatial resolution pixels used in aggregation" layer. Note that the aggregated per-pixel uncertainties represent a pessimistic estimate, as aggregation will reduce the random component of uncertainty as a function of the number of pixels aggregated [32]–[34]. The aggregation of the "output out of range" and the "input out of range" layers is made using the modal function.

© 2017-2024 ACRI-ST

4 Discussion

4.1 Transfer function discussion

As previously mentioned in section 3.6.5 Derivation of calibration functions, the transfer functions given in the Land Products 3, 4 and 5 were only calibrated to be used in the same conditions of their calibration. Indeed, no test or validation was made on other locations than the GBOV sites, or on other period of the year than the one covered by the RMs and SL2P's retrievals matchups. Indeed, the validity of the transfer function is restricted to the sites used within GBOV and their performance may not be reliable over other vegetation types, for instance tropical forests, tundras or mangroves. For those reasons, the given transfer functions are only meant to be used:

- on the corresponding GBOV sites, which means the heterogeneous transfer function for forests sites that are not ICOS sites, the homogeneous transfer function for the grasslands and croplands sites and the ICOS transfer function for the ICOS sites.
- on the ranges covered by the RMs values and SL2P's retrieval values used for the calibration. This is why Land Products processed with values outside of those ranges are immediately flagged as "input out of range" or "output out of range"
- on the period of the year covered by the matchups

4.2 Aggregation methods discussion

The aggregation of the Land Products from the native high resolution (which is approximately 20 to 30 meters) to the CGLS resolution (which is around 300 meters) is made using the modal function for the flags and the mean function for the values and the uncertainties. When the LP values are aggregated with the mean function, a significant part of their variability is lost during the process but by making a mean to aggregate the uncertainty at the same time, this loss of variability is not expressed in the uncertainty. By doing so, the uncertainty in the CGLS resolution pixels is very pessimistic compared to the one in the high-resolution pixels.

Finally, the aggregation gives a value to each low-resolution pixel that are covering at least a portion of a valid native spatial resolution pixel. This means that a low-resolution pixel can have a value that is representative of a very small portion of the area covered by this pixel. Therefore, it is essential to take into account the "valid native spatial resolution pixels used in aggregation (%)" layer. It is recommended to only use for validation the pixels with a "valid native spatial resolution pixels used in aggregation" percentage higher than 50%. Below this percentage, it is estimated that the pixel value is not representative of the zone it is covering. Moreover, a low percentage could be due to the fact that most of the pixels are flagged due to clouds, water, snow or town. We know that those filters are not pixel-perfect and the pixels close to those flagged zones can be outliers that should have been flagged. Knowing that, a low-resolution pixel aggregated with a low valid high resolution pixels percentage should be considered with caution.

© 2017-2024 ACRI-ST

5 Recommendations for use of land products (LPs)

Users are advised to consider the following points when analysing LPs 3, 4 and 5:

- LP values where the input or output is out of range (cf Section 3.8 and 4.1) should be treated with caution, as they are generated by extrapolating beyond the range of the dataset used to establish the calibration function. **It is recommended that such LP values are masked before undertaking further analysis;**

- LPs generated from high spatial resolution imagery acquired outside of the season used to establish the calibration function should be treated with caution. The minimum and maximum day of year (DOY) associated with an LP's calibration function can be found in its README file. **It is recommended that LPs generated from high spatial resolution imagery acquired outside of this range should not used in validation exercises;**

- Because aggregation will reduce the random component of uncertainty as a function of the number of pixels aggregated, **per-pixel uncertainties associated with aggregated LPs will be pessimistic;**

- When using aggregated LPs, a threshold on the percentage of valid native spatial resolution pixels used in aggregation should be applied. **It is recommended that only LP values where at least 50% of the corresponding native resolution pixels are valid are used in validation exercises (cf section 4.2).** A higher threshold may be desired depending on the application;

- Because the RMs used to derive LPs may be sensitive to all elements of the canopy, **attention should be paid to the definitions of RMs and LPs when interpreting the results of validation exercises and comparing with other sattelite land products;**

- The Transfer Functions were computed on specific sites, **they are not meant to be used on other areas,** we indeed never checked them on other areas (cf section 3.6.5 and 4.1)

© 2017-2024 ACRI-ST

Annex A References

[1] M. Weiss *et al.*, "On Line Validation Exercise (OLIVE): A Web Based Service for the Validation of Medium Resolution Land Products. Application to FAPAR Products," *Remote Sens.*, vol. 6, no. 5, pp. 4190–4216, May 2014.

[2] W. Li *et al.*, "A Generic Algorithm to Estimate LAI, FAPAR and FCOVER Variables from SPOT4_HRVIR and Landsat Sensors: Evaluation of the Consistency and Comparison with Ground Measurements," *Remote Sens.*, vol. 7, no. 12, pp. 15494–15516, Nov. 2015.

[3] N. Gobron *et al.*, "Evaluation of fraction of absorbed photosynthetically active radiation products for different canopy radiation transfer regimes: Methodology and results using Joint Research Center products derived from SeaWiFS against ground-based estimations," *J. Geophys. Res.*, vol. 111, no. D13, p. D13110, 2006.

[4] S. T. Gower, C. J. Kucharik, and J. M. Norman, "Direct and Indirect Estimation of Leaf Area Index, fAPAR, and Net Primary Production of Terrestrial Ecosystems," *Remote Sens. Environ.*, vol. 70, no. 1, pp. 29–51, Oct. 1999.

[5] J. T. Morisette *et al.*, "Validation of global moderate-resolution LAI products: a framework proposed within the CEOS land product validation subgroup," *IEEE Trans. Geosci. Remote Sens.*, vol. 44, no. 7, pp. 1804–1817, Jul. 2006.

[6] R. Fernandes *et al.*, "Global Leaf Area Index Product Validation Good Practices," in *Best Practice for Satellite-Derived Land Product Validation*, 2.0., R. Fernandes, S. Plummer, and J. Nightingale, Eds. Land Product Validation Subgroup (Committee on Earth Observation Satellites Working Group on Calibration and Validation), 2014.

[7] F. Baret *et al.*, *VALERI: a network of sites and a methodology for the validation of medium spatial resolution land satellite products*. Avignon, France: Institut National de la Recherche Agronomique, 2005.

[8] J. M. Chen *et al.*, "Derivation and validation of Canada-wide coarse-resolution leaf area index maps using high-resolution satellite imagery and ground measurements," *Remote Sens. Environ.*, vol. 80, no. 1, pp. 165–184, Apr. 2002.

[9] Y. Tian *et al.*, "Multiscale analysis and validation of the MODIS LAI product I. Uncertainty assessment," *Remote Sens. Environ.*, vol. 83, no. 3, pp. 414–430, Dec. 2002.

[10] F. Vuolo, J. Dash, P. J. Curran, D. Lajas, and E. Kwiatkowska, "Methodologies and Uncertainties in the Use of the Terrestrial Chlorophyll Index for the Sentinel-3 Mission," *Remote Sens.*, vol. 4, no. 12, pp. 1112–1133, Apr. 2012.

[11] Y. Chen *et al.*, "Prototyping of LAI and FPAR Retrievals from GOES-16 Advanced Baseline Imager Data Using Global Optimizing Algorithm," *IEEE J. Sel. Top. Appl. Earth Obs. Remote Sens.*, vol. PP, pp. 1–1, 2021.

© 2017-2024 ACRI-ST

[12] J. Sánchez-Zapero, L. Pérez, and B. Fuster, *Copernicus Global Land Operations "Vegetation and Energy" "CGLOPS-1" Scientific Quality Evaluation: LAI, FAPAR FCOVER Collection 300m Version 1*, 1.10. Valencia, Spain: EOLAB, 2018.

[13] L. A. Brown *et al.*, "Evaluation of global leaf area index and fraction of absorbed photosynthetically active radiation products over North America using Copernicus Ground Based Observations for Validation data," *Remote Sens. Environ.*, vol. 247, p. 111935, Sep. 2020.

[14] L. A. Brown, B. Ogutu, F. Camacho, B. Fuster, and J. Dash, "Deriving Leaf Area Index Reference Maps Using Temporally Continuous In Situ Data: A Comparison of Upscaling Approaches," *IEEE J. Sel. Top. Appl. Earth Obs. Remote Sens.*, vol. 14, 2021.

[15] F. Baret, M. Weiss, A. Verger, and B. Smets, *ATBD for LAI, FAPAR and FCOVER from PROBA-V Products at 300m Resolution (GEOV3)*, 1.73. Avignon, France: Institut National de la Recherche Agronomique, 2016.

[16] J. Warren-Wilson, "Estimation of foliage denseness and foliage angle by inclined point quadrats," *Aust. J. Bot.*, vol. 11, no. 1, pp. 95–105, 1963.

[17] J. Miller, "A formula for average foliage density," *Aust. J. Bot.*, vol. 15, no. 1, pp. 141–144, Apr. 1967.

[18] S. G. Leblanc and R. A. Fournier, "Hemispherical photography simulations with an architectural model to assess retrieval of leaf area index," *Agric. For. Meteorol.*, vol. 194, pp. 64–76, Aug. 2014.

[19] USGS, *Product Guide: Landsat 8 Surface Reflectance Code (LaSRC) Product*, 4.2., no. December. Sioux Falls, South Dakota, United States: United States Geological Survey, 2017.

[20] E. Vermote, C. Justice, M. Claverie, and B. Franch, "Preliminary analysis of the performance of the Landsat 8/OLI land surface reflectance product," *Remote Sens. Environ.*, vol. 185, pp. 46–56, Nov. 2016.

[21] U. Müller-Wilm, *Sentinel-2 MSI – Level-2A Prototype Processor Installation and User Manual*. Darmstadt, Germany: Telespazio VEGA, 2016.

[22] USGS, *Landsat 8 Operational Land Imager (OLI) - Thermal Infrared Sensor (TIRS) Solar and View Angle Generation Algorithm Description Document (ADD)*, 2.0. Sioux Falls, South Dakota, United States: United States Geological Survey, 2018.

[23] M. Weiss and F. Baret, *S2ToolBox Level 2 Products: LAI, FAPAR, FCOVER*, 1.1. Avignon, France: Institut National de la Recherche Agronomique, 2016.

[24] J.-B. Feret *et al.*, "PROSPECT-4 and 5: Advances in the leaf optical properties model separating photosynthetic pigments," *Remote Sens. Environ.*, vol. 112, no. 6, pp. 3030–

© 2017-2024 ACRI-ST

3043, Jun. 2008.

[25] S. Jacquemoud and F. Baret, “PROSPECT: A model of leaf optical properties spectra,” *Remote Sens. Environ.*, vol. 34, no. 2, pp. 75–91, Nov. 1990.

[26] W. Verhoef, “Theory of radiative transfer models applied in optical remote sensing of vegetation canopies,” Wageningen Agricultural University, 1998.

[27] W. Verhoef, L. Jia, Q. Xiao, and Z. Su, “Unified Optical-Thermal Four-Stream Radiative Transfer Theory for Homogeneous Vegetation Canopies,” *IEEE Trans. Geosci. Remote Sens.*, vol. 45, no. 6, pp. 1808–1822, Jun. 2007.

[28] N. Djamai, R. Fernandes, M. Weiss, H. McNairn, and K. Goïta, “Validation of the Sentinel Simplified Level 2 Product Prototype Processor (SL2P) for mapping cropland biophysical variables using Sentinel-2/MSI and Landsat-8/OLI data,” *Remote Sens. Environ.*, vol. 225, no. April, pp. 416–430, May 2019.

[29] L. A. Brown *et al.*, “Validation of baseline and modified Sentinel-2 Level 2 Prototype Processor leaf area index retrievals over the United States,” *ISPRS J. Photogramm. Remote Sens.*, vol. 175, no. February, pp. 71–87, May 2021.

[30] L. A. Brown, B. O. Ogutu, and J. Dash, “Estimating Forest Leaf Area Index and Canopy Chlorophyll Content with Sentinel-2: An Evaluation of Two Hybrid Retrieval Algorithms,” *Remote Sens.*, vol. 11, no. 15, p. 1752, Jul. 2019.

[31] M. Stone, “Cross-validatory choice and assessment of statistical predictions,” *J. R. Stat. Soc. Ser. B*, vol. 36, no. 2, pp. 111–147, 1974.

[32] L. A. Brown, J. Dash, A. L. Lidon, E. Lopez-Baeza, and S. Dransfeld, “Synergetic Exploitation of the Sentinel-2 Missions for Validating the Sentinel-3 Ocean and Land Color Instrument Terrestrial Chlorophyll Index Over a Vineyard Dominated Mediterranean Environment,” *IEEE J. Sel. Top. Appl. Earth Obs. Remote Sens.*, vol. 12, no. 7, pp. 2244–2251, Jul. 2019.

[33] F. Camacho, J. Cernicharo, R. Lacaze, F. Baret, and M. Weiss, “GEOV1: LAI, FAPAR essential climate variables and FCOVER global time series capitalizing over existing products. Part 2: Validation and intercomparison with reference products,” *Remote Sens. Environ.*, vol. 137, pp. 310–329, Oct. 2013.

[34] S. Garrigues *et al.*, “Validation and intercomparison of global Leaf Area Index products derived from remote sensing data,” *J. Geophys. Res.*, vol. 113, p. G02028, Jun. 2008.

[35] Joint Committee for Guides in Metrology (JCGM), “Evaluation of measurement data — Guide to the expression of uncertainty in measurement”, Sep. 2008.

[36] S. Liang, J. Wang, "Advanced remote sensing: Terrestrial information extraction and applications", 2nd edition, Chapter 12, 2019.

© 2017-2024 ACRI-ST

[37] Brown, L. A., Morris, H., Leblanc, S., Bai, G., Lanconelli, C., Gobron, N., Meier, C., and Dash, J. (2023), 'HemiPy: A Python module for automated estimation of forest biophysical variables and uncertainties from digital hemispherical photographs', Methods in Ecology and Evolution, 14, pp.2329–2340

[38] Origo, N., Calders, K., Nightingale, J., Disney, M. Influence of levelling technique on the retrieval of canopy structural parameters from digital hemispherical photography. Agric. For. Meteorol. 2017, 237–238, 143–149.

[39] Brown, L.A., Camacho, F., García-Santos, V., Origo, N., Fuster, B., Morris, H., Pastor-Guzman, J., Sánchez-Zapero, J., Morrone, R., Ryder, J. and Nightingale, J., 2021. Fiducial Reference Measurements for Vegetation Bio-Geophysical Variables: An End-to-End Uncertainty Evaluation Framework. Remote Sensing, 13(16), p.3194.

End of document

© 2017-2024 ACRI-ST